SCIENTIFIC REPORTS

OPEN

SUBJECT AREAS:
PHYSICS
MAGNETIC PROPERTIES AND MATERIALS

Received
2 June 2014

Accepted
1 December 2014

Published
18 December 2014

Correspondence and requests for materials should be addressed to Y.T. (y-taguchi@riken.jp)

# Tuning structural instability toward enhanced magnetocaloric effect around room temperature in $MnCo_{1-x}Zn_xGe$

D. Choudhury[1], T. Suzuki[1], Y. Tokura[1,2] & Y. Taguchi[1]

[1]RIKEN Center for Emergent Matter Science (CEMS), Wako 351-0198, Japan, [2]Department of Applied Physics, University of Tokyo, Tokyo 113-8656, Japan.

**Magnetocaloric effect is the phenomenon that temperature change of a magnetic material is induced by application of a magnetic field. This effect can be applied to environmentally-benign magnetic refrigeration technology. Here we show a key role of magnetic-field-induced structural instability in enhancing the magnetocaloric effect for $MnCo_{1-x}Zn_xGe$ alloys ($x$ = 0–0.05). The increase in $x$ rapidly reduces the martensitic transition temperature while keeping the ferromagnetic transition around room temperature. Fine tuning of $x$ around $x$=0.03 leads to the concomitant structural and ferromagnetic transition in a cooling process, giving rise to enhanced magnetocaloric effect as well as magnetic-field-induced structural transition. Analyses of the structural phase diagrams in the $T$-$H$ plane in terms of Landau free-energy phenomenology accounts for the characteristic $x$-dependence of the observed magnetocaloric effect, pointing to the importance of the magnetostructural coupling for the design of high-performance magnetocalorics.**

Cross-coupling between different degrees of freedom often leads to non-trivial material responses to external stimuli, thereby expanding the horizon of exotic materials functions. One such example is the magnetoelectric response in multiferroic materials[1,2], in which magnetic control of polarization and electric reversal of magnetization have recently been demonstrated[3–5]. Another example of the cross-correlation between different degrees of freedom is the magnetostructural coupling, which gives rise to a rich variety of phenomena, such as colossal magnetoresistance (CMR)[6], field-induced structural transitions[7–9], and gigantic magnetocaloric effects[10–12], etc.

Among these phenomena, the magnetocaloric effect has recently attracted much attention due to the anticipation of application to the magnetic refrigeration technique which is environmentally-benign and can be alternative for the gas-compression-based refrigeration. One of the strategies to enhance the magnetocaloric effect, or equivalently the isothermal entropy change $\Delta S$ ($\equiv S(T,H) - S(T,H=0)$) upon the application of magnetic field ($H$), is to combine the lattice degree of freedom with the magnetic one, and to gain the entropy release not only from the magnetic but also from the lattice degree of freedom, associated with the concomitant transition. This principle has been pointed out to be effective for several materials showing a first-order magnetostructural transition, such as $Gd_5Ge_{4-x}Si_x$[13,14] and MnAs[15].

Intermetallic alloys as derived from MnCoGe through chemical modifications are known as another class of materials that show gigantic magnetocaloric effect[16–22]. Pristine MnCoGe compound exhibits a martensitic transformation at around 500 K from a high-temperature hexagonal structure (Fig. 1(a)) to a low-temperature orthorhombic structure (Fig. 1(b))[23]. In the orthorhombic phase, the compound undergoes a ferromagnetic transition at around 340 K, and a neutron diffraction measurement indicates that the values of saturation moment are 2.9 $\pm$ 0.1 and 0.9 $\pm$ 0.2 $\mu_B$ for Mn and Co sites, respectively, which couple ferromagnetically[23]. Large magnetocaloric effects have been reported upon partial substitution of several elements for each site[16–22]. Especially, Zn doping effect at Co site was recently investigated[22], and gigantic values of magnetocaloric effect was reported. However, only intermediate and heavily-doped regions were investigated and it has remained elusive how the magnetocaloric response is enhanced by the coupling between magnetic and structural degrees of freedom as the initially distinct two transitions are merged into a single transition. It also remains unclear how the lattice system responds to magnetic field as the relation between structural and magnetic transition temperatures are tuned systematically. In this Article, we reveal, based on extensive investigations on $MnCo_{1-x}Zn_xGe$ with finely controlled Zn concentration including lightly doped materials, that the lattice

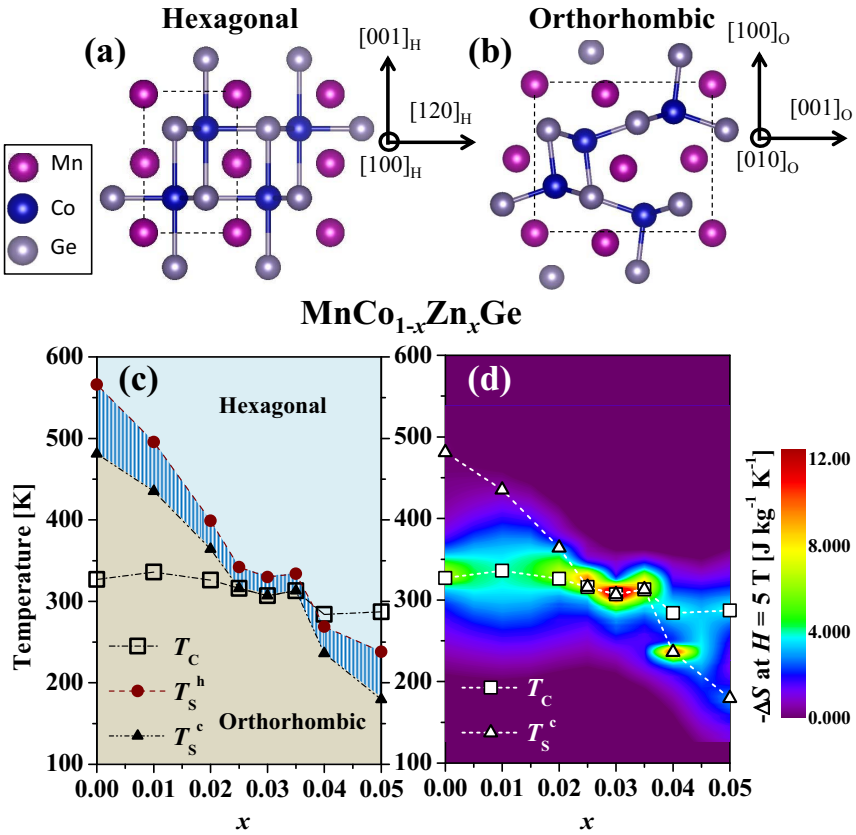


**Figure 1 | Magnetic- and structural-phase-diagram.** Schematic figure of the (a) hexagonal and (b) orthorhombic structure of MnCoGe as viewed along the same spatial direction. Dashed lines indicate unit cells for the respective structures. The directions of crystal axes are indicated with conventional hexagonal and orthorhombic settings, respectively. (c) Magnetic and structural phase diagram of $MnCo_{1-x}Zn_xGe$. The hatched area indicates the thermal hysteresis related to the structural transition. $T_S^h$ and $T_S^c$ denote structural transition temperatures on heating and cooling, respectively. $T_C$ indicates ferromagnetic transition temperature on cooling. (d) Contour plot of the magnetocaloric effect, or equivalently isothermal entropy change (-$\Delta S$), of $MnCo_{1-x}Zn_xGe$ for a field change from 0 T to 5 T which was measured in the cooling run.

structure is controllable with $H$ and that the conspicuous enhancement of the magnetocaloric effect is observed as the structural instability is tuned to the ferromagnetic one around room temperature (Figs. 1(c) and (d)). To understand the physics behind the enhanced magnetocaloric effect, the magnetostructural phase diagram was analyzed in terms of Landau free energy, and we found an intimate correlation between magnetocaloric effect and the phenomenological magnetostructural coupling strength. In addition, both the magnetocaloric values and magnetostructural coupling parameters are found to exhibit characteristic asymmetric $x$-variation between lightly-doped and heavily-doped regions, depending on the relation between structural and magnetic transition temperatures.

## Results

In Fig. 2(a), we show the temperature dependence of magnetization of selected samples of $MnCo_{1-x}Zn_xGe$ below 400 K in $H = 1$ T. In this temperature range, undoped compound possesses orthorhombic structure, and exhibits the ferromagnetic transition at $T_C = 327$ K with a low-temperature saturation moment of 4.2 $\mu_B$/f.u. in accord with a previous report[23]. As the partial substitution of Zn proceeds, the temperature dependence of magnetization exhibits hysteresis behavior for $x \geq 0.03$ while ferromagnetic transition temperature $T_C$ remains almost unchanged at around 300 K. As shown below, the hysteresis in the magnetization corresponds to the structural transition, thus the structural transition temperature is rapidly reduced as $x$ is increased. For $x$=0.03, its structural transition temperature ($T_S^c$) in the cooling process coincides with $T_C$, giving rise to a first-order coupled magnetic and structural transition. In the heating process, $T_C$ occurs first, followed by the structural transition ($T_S^h$). Both the $x$=0.04 and 0.05 compounds exhibit ferromagnetic transitions at around 285 K in the hexagonal phase, and structural transitions occur at lower temperatures ($T_S^c$ and $T_S^h$) than $T_C$. This observation is most clearly evidenced for $x$=0.04 by the temperature dependence of normalized X-ray diffraction intensity of the hexagonal phase which is also plotted in Fig. 2(a). The structural transition from the high-temperature hexagonal phase to the low-temperature orthorhombic phase is accompanied by an increase in magnetization, as clearly observed for ferromagnetic alloys with $x$=0.04 and 0.05. In the case of paramagnetic phase for $x$=0, the structural transition manifests itself in the temperature dependence of magnetization as tiny temperature hysteresis between $T_S^h$~570 K and $T_S^c$~480 K (not shown). The structural transition temperatures $T_S^h$ and $T_S^c$ for $x$=0.02 lie above $T_C$ as well, while the alloy in the orthorhombic phase undergoes the ferromagnetic ordering at $T_C = 326$ K.

The structural transition temperatures for $x$=0.04, as estimated from the changes in the normalized X-ray diffraction intensity $I_H/(I_O + I_H)$ during heating- and cooling-runs shown in Fig. 2(a), are found to coincide well with the position of temperature-hysteresis in magnetization data as defined by the maxima in its temperature-deriavative. The structural transition temperatures in the absence of magnetic field were also confirmed by differential scanning calorimetry method. For $0.025 \leq x \leq 0.035$, while a coupled magnetic and structural transition is realized on cooling, the magnetic transition occurs at a lower temperature than the structural transition on heating. Based on these temperature-dependent structural and magnetic data, we constructed the phase diagram of $MnCo_{1-x}Zn_xGe$, as shown in Fig. 1(c).

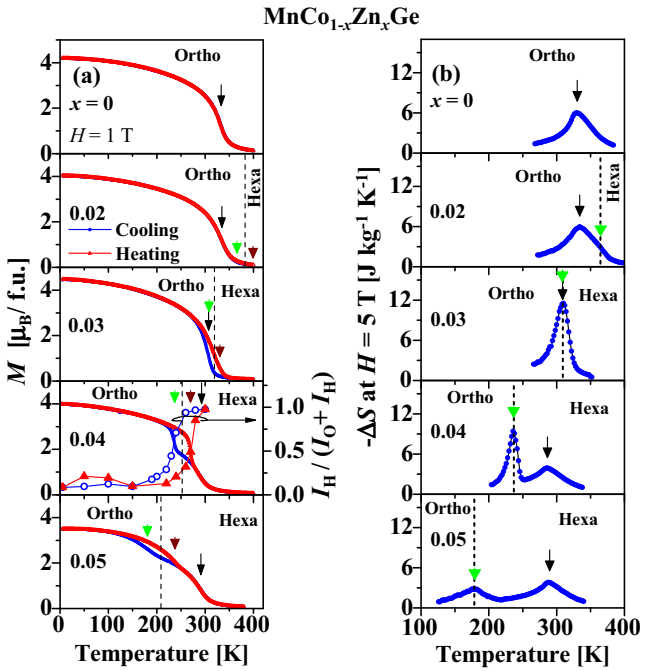


**Figure 2 | Magnetization and magnetocaloric effect.** Temperature dependence of (a) magnetization at $H = 1$ T and (b) magnetocaloric effect ($-\Delta S$) for a field change from 0 T to 5 T for selected samples of $MnCo_{1-x}Zn_xGe$. Also shown for $x$=0.04 in (a) are temperature dependence of normalized intensity $I_H/(I_O + I_H) \equiv I^H_{[110]}/(I^O_{[211]} + I^H_{[110]})$, where $I^H_{[110]}$ and $I^O_{[211]}$ are the intensities of [110] and [211] X-ray diffraction peaks of hexagonal and orthorhombic phases, respectively, measured in a heating run (closed triangle) and in a cooling run (open circle) under zero magnetic field. The black, green and brown arrows indicate the magnetic transition ($T_C$) in cooling process, structural transitions in cooling ($T_S^c$) and heating ($T_S^h$) processes, respectively.

As clearly seen in this phase diagram, the structural transition temperature can be significantly and systematically reduced by increasing $x$. This rapid reduction of the structural transition temperature may be accounted for in terms of the difference in electronegativity of Co and Zn; Doping a less-electronegative ion at Co site, or a more-electronegative ion at Mn site, should lead to a stronger Mn-Mn bond, thereby reducing the martensitic structural transition temperature, similar to the case of MnNiGe[24]. (We note that Co and Zn have Pauling-electronegativity of 1.88 and 1.65, respectively.) On the basis of the relationship between the structural and magnetic transition temperatures, the whole phase diagram can be considered as consisting of three different $x$-regions. In the first $x$-region of $0 \le x \le 0.02$, the structural transition temperature remains higher than the magnetic transition temperature $T_C$, and rapidly decreases with increasing $x$. In the second $x$-region of $0.025 \le x \le 0.035$, a concomitant structural and magnetic transition occurs in the cooling run, and this temperature remains nearly constant irrespective of $x$-values, suggesting a strong coupling between the lattice and magnetism. Associated with this magnetostructural clamping behavior, a significant reduction of structural-hysteresis is also observed. In the third $x$-region of $0.04 \le x \le 0.05$, the clamping between structural and magnetic transitions is released and the structural transition temperatures, $T_S^h$ and $T_S^c$, become lower than $T_C$.

Given the global phase diagram from undoped to heavily-doped regions, we next investigate the magnetocaloric effect of the $MnCo_{1-x}Zn_xGe$ alloys. In Fig. 2(b), we show temperature dependence of $-\Delta S$ deduced via Maxwell's relation from isothermal $M$-$H$ measurements that are performed in the cooling run. For $x$=0.04 and 0.05, $-\Delta S$ shows two-peak structure, higher one corresponding to $T_C$ and the lower one to $T_S^c$, similar to the previous report[22], although the higher-temperature peak corresponding to $T_C$ is more pronounced in our case. On the other hand, $-\Delta S$ for $x$=0 exhibits a single peak corresponding to $T_C$ in this temperature range ($T_S^c$=481 K is out of the temperature range displayed in Fig. 2(b)). For $x$=0.02, a very weak shoulder-like structure is barely discernible at the higher temperature side of the peak at $T_C$. For $x$=0.03, the two peaks merge to give rise to a moderately large $-\Delta S$ value of 11.5 J kg$^{-1}$ K$^{-1}$. Another relevant quantity to evaluate the applicability of a magnetocaloric material is the relative-cooling-power (RCP)[25], which is defined as $RCP \equiv -\Delta S_{peak} \times T_{FWHM}$, where $-\Delta S_{peak}$ is the peak-value of $-\Delta S$ and $T_{FWHM}$ is the full-width-at-half-maximum of $-\Delta S$ curve as a function of temperature[12]. The alloy with $x$=0.03 exhibits a large RCP value of 305 J kg$^{-1}$ (with $-\Delta S_{peak}$ value of 11.5 J kg$^{-1}$ K$^{-1}$ and $T_{FWHM}$ of approximately 27 K). We note that this is the largest RCP value among the MnCoGe-related compounds, in which a smaller value of $T_{FWHM}$, hence leading to smaller RCP values, has been observed[17,18,20]. This value of RCP of the present material is slightly smaller than some of the most promising magnetocaloric materials, such as $Gd_5Si_2Ge_2$, Gd, $MnFeP_{0.5}As_{0.5}$, and $LaFe_{10.4}Co_{0.8}Si_{1.8}$ with RCP values of 535, 410, 490, and 600 J kg$^{-1}$, respectively[12]. Another point to be noted in Fig. 2(b) that was not revealed in the previous study[22] is the asymmetry related to $-\Delta S$ values at $T_S^c$; The $-\Delta S$ value for $x$=0.04 at $T_S^c$ which is lower than $T_C$ is clearly larger than that for $x$=0.02 at $T_S^c$ which is higher than $T_C$, in spite of the comparable values of $|T_S^c - T_C|$. Namely, once the magnetic order is established, the effect of $H$ on the structural transition is significant while much less in the absence of the magnetic order. The magnetocaloric values for all the $MnCo_{1-x}Zn_xGe$ materials investigated here are displayed in Fig. 1(d) as a contour plot. Clearly, the magnetocaloric effect shows conspicuous enhancement for $0.025 \le x \le 0.035$ with concomitant magnetostructural transition, and also asymmetric behavior with respect to this $x$-region.

To gain more insight into the observed magnetocaloric effects, we have investigated the $H$-effect on the structural transitions for all $x$ members. In Fig. 3(a), we show the temperature-dependence of magnetization of the $x$=0.03 alloy for several values of $H$. As $H$ is progressively increased, the temperature at which magnetization begins to increase moves rapidly to the higher temperature. The values of $T_C$, $T_S^c$, and $T_S^h$ were determined from the temperature-derivative of magnetization data that are shown in Fig. 3(b), and plotted in Fig. 3(c). (It should be noted that this method is quite accurate to estimate the field-dependence of first-order transition temperature whereas it gives only a rough estimate for a second-order magnetic transition.) We find that the $x$=0.03 alloy undergoes concomitant magnetic- and structural-transition ($T_C = T_S^c$) on cooling for all the values of $H$, while on heating they coincide with each other only for $H \ge 4$ T. For $H < 4$ T, $T_C$ appears to be lower than $T_S^h$, which is the origin of non-parallel shift of the $M$-$T$ curves in Fig. 3(a) between cooling- and heating-runs at $H$ = 0.3 T and 1 T, in contrast to the data for $H > 4$ T. In the presence of $H$, the gain in Zeeman energy is larger for the orthorhombic phase due to its larger magnetization than for the hexagonal phase. This gives rise to an increase of the structural transition temperature ($T_S^c$ and $T_S^h$), stabilizing the orthorhombic phase in a wide temperature range under $H$. For this $x$=0.03 compound, shift rate of $T_S^c$ ($dT_S^c/dH$) is as large as 1.1 K/T. From the similar measurements for other samples, we determined the shift rate of $T_S^c$ as a function of $x$, and plotted in Fig. 4(c).

In order to estimate the phenomenological magnetostructural coupling strength, we have analyzed the $T$-$H$ phase diagram by using Landau free-energy scheme, which has been applied for studying magnetostructural transitions in shape-memory alloys, for example, in $Ni_2Mn_{1-x}Cu_xGa$[26]. The Landau free-energy ($f$) expansion for coupled magnetic and structural degrees of freedom is expressed[8,27,28] as

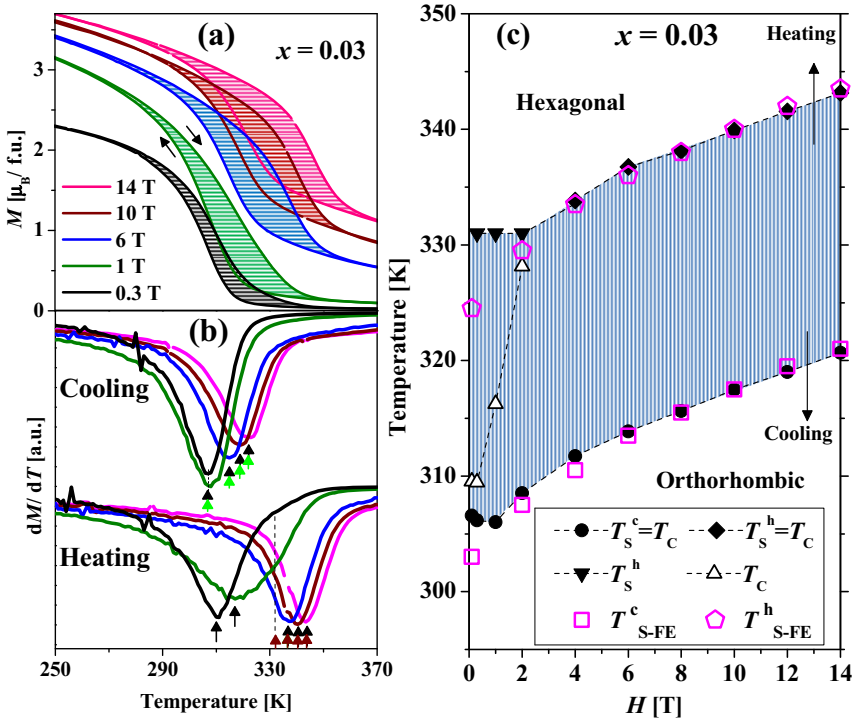


**Figure 3 | Magnetic-field-induced structural instability.** Temperature dependence of magnetization (a) and $\frac{dM}{dT}$ (b) of $x$=0.03 alloy at several magnetic fields measured in both heating and cooling processes (as indicated with arrows in (a) for 1 T case). The $\frac{dM}{dT}$ plots between heating and cooling runs are vertically shifted for the purpose of clarity. Hatching in (a) indicates thermal hysteresis. The black, green and brown arrows in (b) indicate the magnetic transition ($T_C$), structural transitions in cooling ($T_S^c$) and heating ($T_S^h$) processes, respectively. The compound undergoes a concomitant magnetic and structural transition on cooling for all the $H$ values while only for $H \geq 4$ T on heating. In the cooling run, $T_C$ (and $T_S^c$) are almost the same for 0.3 T and 1 T. For $H$ = 0.3 T and 1 T, the structural transition in the heating run occurs at almost the same temperature and higher than the corresponding magnetic transition, causing the deviation from a simple parallel shift of the magnetization data between heating and cooling runs in (a) and the broadness of $\frac{dM}{dT}$ in (b). (c) Experimentally observed values of $T_C$, $T_S^c$ and $T_S^h$ are plotted against magnetic field. The structural transition temperatures in the cooling ($T^c_{S-FE}$) and heating ($T^h_{S-FE}$) processes as estimated from Landau free-energy analyses are also plotted. Hatching indicates the thermal hysteresis of the structural transition.

$$f = f_0 + \frac{A}{2}(T - T_C^0)M^2 + \frac{T_\beta}{4}M^4 - MH + \frac{A'}{2}(T - T_S^0)Q^2 - \frac{T_{\beta'}}{4}Q^4 + \frac{T_\gamma}{6}Q^6 - \frac{T_\eta}{2}M^2Q^2 \quad (1)$$

where $f_0$ is a constant part of the free-energy, $A$, $T_\beta$, $A'$, $T_{\beta'}$, $T_\gamma$, and $T_\eta$ are parameters. $T_C^0$ ($T_S^0$) is the magnetic (structural) transition temperature on cooling without $H$ (magnetostructural coupling). $M$ and $Q$ are the normalized magnetization and lattice-distortion index; $Q$=0 for the hexagonal phase and 1 for the orthorhombic phase. Based on this free-energy expansion, we obtained the structural transition temperatures $T^h_{S-FE}$ and $T^c_{S-FE}$ (see Methods section for details), which are displayed in Fig. 3(c). This analysis enables us to deduce a magnetostructural coupling strength $T_\eta$ corresponding to the $M^2Q^2$ term for a given $x$ composition. We performed the same analysis for all the investigated alloys; the $x$-dependence of the obtained $T_\eta$ is shown in Fig. 4(d). Here, $T_\eta$ is expressed in unit of energy since $M$ and $Q$ are normalized.

As clearly seen, $T_\eta$ attains the largest values in the intermediate $x$-region of $0.025 \leq x \leq 0.035$. This composition range almost coincides with the range for which the obtained -$\Delta S$ values are maximized, as plotted in Fig. 4(a). Furthermore, the characteristic asymmetry in the $x$-dependence of the -$\Delta S$ values at $T_S^c$, namely small -$\Delta S$ for $x \leq 0.02$ and large -$\Delta S$ for $x \geq 0.04$, is similar with that of the obtained $T_\eta$ values, as seen in Fig. 4(a) and (d). These observations clearly show the intimate correlation between these two quantities. When the coupling constant $T_\eta$ (biquadratic term of free-energy) is large, application of magnetic field can induce large lattice distortion via the field-induced magnetization near $T_C$, giving rise to the large entropy change from the lattice degrees of freedom in addition to the magnetic entropy change, accounting for large -$\Delta S$ values. Also, the thermal hysteresis width of the structural transition becomes small for this composition range, as shown in Fig. 4(b). The coupling term $-\frac{T_\eta}{2}M^2Q^2$ stabilizes the distorted (orthorhombic) phase when there is a finite magnetization (regardless of whether it is spontaneous or induced moment), giving rise to an increase in transition temperatures from $T_S^c = T_S^0$ to $T_S^0 + T_\eta \frac{[M^c]^2}{A'}$, and from $T_S^h = T_S^0 + \frac{T_{\beta'}^2}{4T_\gamma A'}$ to $T_S^0 + \frac{T_{\beta'}^2}{4T_\gamma A'} + T_\eta \frac{[M^h]^2}{A'}$ for cooling and heating process, respectively, where $M^c$ and $M^h$ denote the magnetization at $T_S^c$ and $T_S^h$. (Here, $T_S^c$ and $T_S^h$ in the presence of the magnetostructural coupling term should be considered to be determined from the above equation self-consistently.) Therefore, thermal hysteresis changes from $\frac{T_{\beta'}^2}{4T_\gamma A'}$ to $\frac{T_{\beta'}^2}{4T_\gamma A'} + T_\eta\left[[M^h]^2 - [M^c]^2\right]/A'$. Since $[[M^h]^2 - [M^c]^2] < 0$ holds in general, the coupling between magnetization and lattice degrees of freedom reduces the hysteresis width; the hysteresis becomes smaller when the coupling constant $T_\eta$ is larger.

The controllability of structure by a magnetic field is represented by the shift rate of $T_S^c$, and its $x$-dependence is plotted in Fig. 4(c). It is

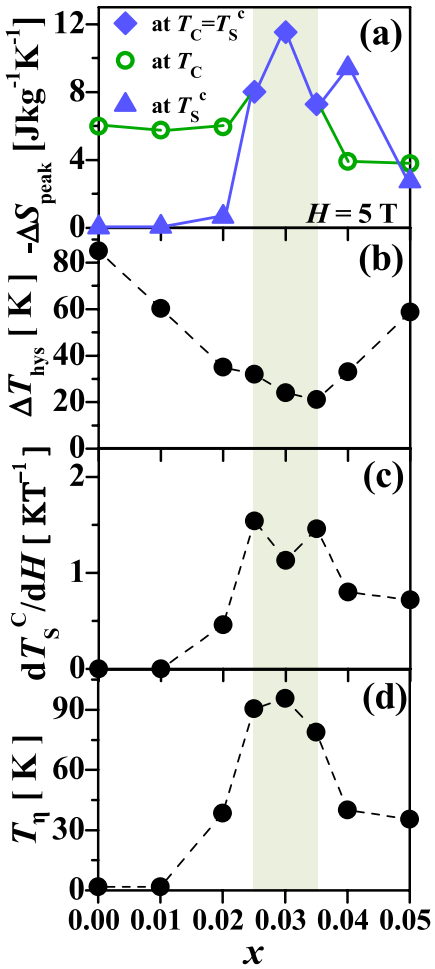


**Figure 4 | Correlation between magnetocaloric effect and magnetostructural coupling strength.** Zn concentration ($x$) dependence of (a) the peak value of magnetocaloric effect, or isothermal entropy change (-$\Delta S$), for a field change from 0 T to 5 T, at $T_C$ and $T_S^c$, (b) the thermal hysteresis related to the structural transition ($\Delta T_{hys}$), (c) the shift rate of $T_S^c$ with application of magnetic field $H$ ($dT_S^c/dH$) and (d) the magnetostructural coupling strength ($T_\eta$) as estimated from Landau free-energy analyses. The solid and dashed lines are the guide to the eyes, and the shaded region corresponds to the region where magnetic and structural transitions occur concomitantly.

reasonable that this quantity and the magnetostructural coupling constant $T_\eta$ plotted in Fig. 4(d) show very similar $x$-dependence. Field-induced structural transition has also manifested itself in the $M$-$H$ curves as (very gradual) metamagnetic-like and irreversible behavior. This behavior was observed in alloys with $T_C \geq T_S$ at around $T_S$, and the magnitude of the field-induced magnetization enhancement associated with the structural transition becomes smaller as $x$ becomes larger, in accord with the $x$-dependence of $T_\eta$ in this $x$-range.

In summary, a series of $MnCo_{1-x}Zn_xGe$ alloys are systematically synthesized and their magnetic and structural phase diagram is revealed. The increase in $x$ rapidly reduces the structural transition temperature. As $x$ is finely tuned to the intermediate $x$ compositions ($0.025 \leq x \leq 0.035$), enhanced magnetocaloric effect at the concomitant magnetostructural transitions as well as considerable change of structural transition temperatures is observed upon applying magnetic field. The structural phase diagram in the $T$-$H$ plane is analyzed in terms of Landau free-energy scheme to obtain the magnetostructural coupling constant, and the characteristic $x$-dependence of the magnetocaloric effect at the structural transition temperature is found to closely correlate with the variation in the coupling strength. The link between the magnetocaloric effect and magnetostructural coupling as revealed in this work will be useful for designing magnetocaloric materials, and also point to the importance of the interplay between the magnetic and lattice degrees of freedom to obtain large magnetocaloric responses in general. Reducing the thermal hysteresis will be a future problem to be overcome.

## Methods

**Sample synthesis and characterization.** $MnCo_{1-x}Zn_xGe$ samples were synthesized with solid-state synthesis route by mixing Mn, Co, Zn and Ge metallic powders and sintering them in $Al_2O_3$ crucibles placed inside evacuated quartz ampoules, at 975°C for 16 hours and then at 1050°C for 2 hours, with intermittent grinding and slow-cooling. Co, Zn and Ge powders were mixed in stoichiometric amounts while 1.1 times the stoichiometric amount of Mn was taken in order to account for the loss of Mn during sintering. Chemical homogeneity and compositions of the samples were checked by using energy dispersive X-ray (EDX) analysis. EDX results suggest approximately 3% deficiency in Co content compared to the nominal compositions. The cell volume at room temperature was found to remain nearly constant as $x$ is varied, perhaps due to similar atomic radii of Co and Zn.

**Measurements of structural and magnetocaloric properties.** Low-temperature X-ray diffraction measurements were carried out in vacuum atmosphere to investigate the structural transitions for selected samples. Magnetocaloric values were evaluated from isothermal $M$-$H$ measurements by using Maxwell's relation, following the loop process[29], which has proved to be indispensable to evaluate magnetocaloric quantities accurately for first-order as well as second-order transitions[29,30].

**Analyses of $T$-$H$ phase diagram based on Landau free energy expansion.** We first assumed a set of parameters ($A'$, $T_\beta'$, $T_\gamma$, and $T_\eta$) for the last four terms in the free-energy $f$ expansion of Eq. (1), and using the experimental $T$-dependent values of $M$ at a certain $H$ for the last $M^2Q^2$ term, examined the shape of the free energy $f$ as function of the distortion $Q$ for a certain value of $T$. We then changed $T$ value, and looked for $T_{S-FE}$ as the temperature $T$ where the shape of $f$ as a function of $Q$ is such that the energy barrier between the local-minimum and global-minimum of $f$ goes to zero. In the heating-process, the structural transition temperature ($T^h_{S-FE}$) is determined as the temperature where the energy-barrier for the system to change from the local-minimum of the free-energy at $Q$=1 (the orthorhombic phase) to the global-minimum at $Q$=0 (the hexagonal phase) becomes zero to cause a first-order phase transition. In the cooling-process, the transition temperature ($T^c_{S-FE}$) is similarly estimated as the temperature where the energy-barrier to prevent the system from changing from local-minimum at $Q$=0 to global-minimum at $Q$=1 vanishes. We then compared these values of $T_{S-FE}$ with the experimental values of $T_S$. We changed parameter values of $A'$, $T_\beta'$, $T_\gamma$, and $T_\eta$ and repeated the procedure so that calculated $T_{S-FE}$ and experimental values of $T_S$ show good agreement with each other. We used the same set of optimized parameter ($A'$, $T_\beta'$, $T_\gamma$, and $T_\eta$) values for both the heating and cooling processes, and for different magnetic field strengths and repeated the same procedures for different $x$ compositions.


1. Cheong, S. W. & Mostovoy, M. Multiferroics: a magnetic twist for ferroelectricity. *Nature Mat.* **6**, 13–20 (2007).
2. Tokura, Y. & Seki, S. Multiferroics with Spiral Spin Orders. *Adv. Mat.* **22**, 1554–1565 (2010).
3. Kimura, T. *et al.* Magnetic control of ferroelectric polarization. *Nature* **426**, 55–58 (2003).
4. Hur, N. *et al.* Electric polarization reversal and memory in a multiferroic material induced by magnetic fields. *Nature* **429**, 392–395 (2004).
5. Tokunaga, Y., Taguchi, Y., Arima, T. & Tokura, Y. Electric-field-induced generation and reversal of ferromagnetic moment in ferrites. *Nature Phys.* **8**, 838–844 (2012).
6. Tokura, Y. Critical features of colossal magnetoresistive magnanites. *Rep. Prog. Phys.* **69**, 797–851 (2006).
7. Asamitsu, A., Moritomo, Y., Tomioka, Y., Arima, T. & Tokura, Y. A structural phase transition induced by an external magnetic field. *Nature (London)* **373**, 407–409 (1995).
8. Asamitsu, A., Moritomo, Y., Kumai, R., Tomioka, Y. & Tokura, Y. Magnetostructural phase transitions in $La_{1-x}Sr_xMnO_3$ with controlled carrier density. *Phys. Rev. B* **54**, 1716–1723 (1996).
9. Kainuma, R. *et al.* Magnetic-field-induced shape recovery by reverse phase transformation. *Nature* **439**, 957–960 (2006).
10. Gschneidner Jr., K. A., Pecharsky, V. K. & Tsokol, A. O. Recent developments in magnetocaloric materials. *Rep. Prog. Phys.* **68**, 1479–1539 (2005).
11. Brück, E. Developments in magnetocaloric refrigeration. *J. Phys. D : Appl. Phys.* **38**, R381–R391 (2005).
12. Phan, M. H. & Yu, S. C. Review of the magnetocaloric effect in manganite materials. *J. Magn. Magn. Mater.* **308**, 325–340 (2007).
13. Pecharsky, V. K. & Gschneidner Jr., K. A. Giant Magnetocaloric Effect in $Gd_5(Si_2Ge_2)$. *Phys. Rev. Lett.* **78**, 4494–4497 (1997).

14. Choe, W. *et al.* Making and Breaking Covalent Bonds across the Magnetic Transition in the Giant Magnetocaloric Material $Gd_5(Si_2Ge_2)$. *Phys. Rev. Lett.* **84**, 4617–4620 (2000).
15. Wada, H. & Tanabe, Y. Giant magnetocaloric effect of $MnAs_{1-x}Sb_x$. *Appl. Phys. Lett.* **79**, 3302–3304 (2001).
16. Hamer, J. B. A. *et al.* Phase diagram and magnetocaloric effect of $CoMnGe_{1-x}Sn_x$ alloys. *J. Magn. Magn. Mater.* **321**, 3535–3540 (2009).
17. Trung, N. T., Zhang, L., Buschow, K. H. J. & Brück, E. Giant magnetocaloric effects by tailoring the phase transitions. *Appl. Phys. Lett.* **96**, 172504 (2010).
18. Trung, N. T. *et al.* From single- to double-first-order magnetic phase transition in magnetocaloric $Mn_{1-x}Cr_xCoGe$ compounds. *Appl. Phys. Lett.* **96**, 162507 (2010).
19. Ma, S. C. *et al.* Large room temperature magnetocaloric effect with negligible magnetic hysteresis losses in $Mn_{1-x}V_xCoGe$ alloys. *J. Magn. Magn. Mater.* **324**, 135–139 (2012).
20. Samanta, T., Dubenko, I., Quetz, A., Stadler, S. & Ali, N. Giant magnetocaloric effects near room temperature in $Mn_{1-x}Cu_xCoGe$. *Appl. Phys. Lett.* **101**, 242405 (2012).
21. Li, G. J. *et al.* Phase diagram, ferromagnetic martensitic transformation and magnetoresponsive properties of Fe doped MnCoGe alloys. *J. Magn. Magn. Mater.* **332**, 146–150 (2013).
22. Samanta, T., Dubenko, I., Quetz, A., Stadler, S. & Ali, N. Large magnetocaloric effects over a wide temperature range in $MnCo_{1-x}Zn_xGe$. *J. Appl. Phys.* **113**, 17A922 (2013).
23. Niziol, S., Bombik, A., Baźela, W., Szytula, A. & Fruchart, D. Crystal and magnetic structure of $Co_xNi_{1-x}MnGe$ system. *J. Magn. Magn. Mater.* **27**, 281–292 (1982).
24. Liu, E. *et al.* Stable magnetostructural coupling with tunable magnetoresponsive effects in hexagonal ferromagnets. *Nat. Commun.* **3**, 873 (2012).
25. Wood, M. E. & Potter, W. H. General analysis of magnetic refrigeration and its optimization using a new concept: maximization of refrigerant capacity. *Cryogenics* **25**, 667–683 (1985).
26. Kataoka, M. *et al.* Martensitic transition, ferromagnetic transition, and their interplay in shape memory alloys $Ni_2Mn_{1-x}Cu_xGa$. *Phys. Rev. B* **82**, 214423 (2010).
27. Lifshitz, E. M. & Pitaevskii, L. P. *in Statistical Physics,* edited by Landau, L. D. & Lifstitz, E. M. *Course Of Theoretical Physics*. **Vol – 3**, Chapter 14 (Pergamon, Oxford, 1978).
28. Imry, Y. On the statistical mechanics of coupled order parameters. *J. Phys. C : Solid State Phys.* **8**, 567–577 (1975).
29. Caron, L. *et al.* On the determination of the magnetic entropy change in materials with first-order transitions. *J. Magn. Magn. Mater.* **321**, 3559–3566 (2009).
30. Porcari, G. *et al.* Convergence of direct and indirect methods in the magnetocaloric study of first order transformations: The case of Ni-Co-Mn-Ga Heusler alloys. *Phys. Rev. B* **86**, 104432 (2012).


## Acknowledgments

The work is supported by Funding program for World Leading Innovative R&D on Science and Technology (FIRST) on "Quantum Science on Strong Correlation" from JSPS.

## Author contributions

D.C. performed syntheses and characterizations of the samples, and investigated their magnetic and magnetocaloric properties. D.C. and T.S. carried out the temperature-dependent X-ray diffraction experiments. The results were discussed and analyzed by D.C., Y. Taguchi, and Y. Tokura. D.C, Y. Tokura, and Y. Taguchi wrote the manuscript and all authors reviewed the manuscript.

## Additional information

**Competing financial interests:** The authors declare no competing financial interests.

**How to cite this article:** Choudhury, D., Suzuki, T., Tokura, Y. & Taguchi, Y. Tuning structural instability toward enhanced magnetocaloric effect around room temperature in $MnCo_{1-x}Zn_xGe$. *Sci. Rep.* **4**, 7544; DOI:10.1038/srep07544 (2014).